JOURNAL OF GUIDANCE, CONTROL, AND DYNAMICS
Vol. 16, No. 1, January-February 1993

Trajectory Design, Feedforward, and Feedback Stabilization of Tethered Spacecraft Retrieval

Eric J. Fleurisson* and Andreas H. von Flotow†
Massachusetts Institute of Technology, Cambridge, Massachusetts 02139
and
Darryll J. Pines‡
Lawrence Livermore National Laboratory, University of California, Livermore, California 94551

This paper focuses on the final 2 km of retrieval of a tethered subsatellite (TSS) to the Space Shuttle. From each initial condition a nominal retrieval trajectory is determined, which is implemented with the tether reel and requires nominally zero thrusting. The retrieval dynamics of the TSS are unstable, and open loop retrieval by itself is not practical. Consequently, a loop structure is designed that combines feedforward information with thruster actuated feedback stabilization. The tether-normal thrusters mounted on the subsatellite are used to stabilize the in-plane and out-of-plane dynamics along the precomputed trajectory. A Kalman filter is used to estimate pitch and pitch rate from a noisy pitch sensor. This whole design yields fast retrievals, limited primarily by constraints on docking speed and tether tension. Thruster fuel use is driven by sensor noise, rather than by the need to remove system angular momentum. Numerical results clearly indicate that, to limit fuel use, system pitch attitude must be measured with a resolution much better than the 2 deg currently planned.

I. Introduction

IN the past decade the dynamics and control of a subsatellite tethered to the Space Shuttle by a taut, low-mass, long tether have received a considerable amount of attention.[1,2] This system is often referred to as the tethered subsatellite system (TSS), where the orbiter represents the primary launch vehicle from which the tether is deployed or retrieved. Early models of this system have evolved from simple point-mass descriptions to models that include in-plane and out-of-plane deformations of the tether and that retain some pertinent dynamics of the orbiter.[1,3,4]

Because a typical mission involves deployment, stationkeeping, and retrieval, the control problem can be divided into at least three phases, each requiring a different control strategy. Of the three phases, the retrieval phase is the most interesting since it is inherently unstable in many modes of motion, including the simplest pitch and roll attitude motion, the tether length motion, and possibly tether deformation modes. Some of these modes can be stabilized by using the tether-reel-in rate for most of the retrieval; however, within about 2 km this leads to very slow retrievals due to the weak nature of the gravity gradient torque.[5-7] Such slow retrievals are the consequence of specifying a constant equilibrium pitch angle some distance—say, 30 deg—from the local vertical and employing only gravity gradient pitch torques to remove the system angular momentum.

Tether-normal thrusting can be used to remove the system angular momentum during retrieval. If such thrusting is applied to only one of the subsatellites (presumably the less massive one), then the velocity change Δv required for a tether length change ΔL is $\Delta v = \omega \Delta L$, where ω is the orbital rate. This requires a Δv of 2 m/s for a 2-km retrieval in low Earth orbit (LEO). Tether-normal thrusting can also be used to stabilize the unstable perturbational dynamics during retrieval. In the work reported here, instead of attempting to use the thrusters to stabilize along some arbitrary retrieval path, a retrieval path is selected with large and time-varying pitch excursions. The retrieval path, though unstable, satisfies the pitch dynamics; without thrusting, stored angular momentum is removed by gravity gradient torques. The nominal retrieval path is established by commanding a specific length-rate profile. Tether-normal thrusting is used only to stabilize this unstable trajectory, not to remove the angular momentum stored in the deployed system. The loop structure envisioned is sketched in Fig. 1; for a given initial condition a retrieval trajectory is planned. This retrieval trajectory consists of time histories for tether length L and pitch angle θ (roll angle ϕ is always commanded to zero.) The length trajectory is implemented with the tether reel, whereas the pitch trajectory becomes a time-varying set point for a regulator feedback loop that uses tether-normal thrusters.

Feedforward trajectories from arbitrary initial conditions and for docking conditions of zero pitch angle (aligned with the local vertical), zero pitch rate, and limited impact velocity are generated. Retrievals for which the tethered system is allowed to tumble are excluded. The feedforward trajectories presented are motivated by optimal control arguments, and methods of optimal control are used to discover the existence of an *invariant final approach path* or *docking corridor*, which the subsatellite must follow in the final minutes (8 min in LEO) if it is to dock with the specified final conditions. Retrieval trajectories for arbitrary initial conditions are then synthesized such that the system is brought onto this docking corridor in a sensible way.

Feedback stabilization of the perturbational dynamics about these nominal retrieval trajectories is accomplished using tether-normal thrusters. Pines, von Flotow, and Redding[8] investigated both an ad hoc phase plane control scheme and a more formal sliding mode control methodology for stabilizing

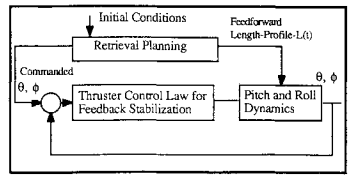

Fig. 1 Block diagram of the retrieval control logic.

Received May 30, 1991; revision received June 2, 1992; accepted for publication June 19, 1992.

*Associate Professor, Department of Aeronautics and Astronautics.
†Graduate Research Assistant, Department of Aeronautics and Astronautics.
‡Member of Technical Staff, Mechanical Engineering Division.

the retrieval dynamics of the TSS by using the orbiter's thrusters as control inputs. They show that on-off firing of the orbiter's thrusters in the first approach leads to stable limit cycles for both pitch and roll dynamics, whereas the sliding mode method achieves remarkable theoretical performance for continuous thruster firing. Misra et al.[9] used tether-normal thrusting (assumed to be continuous) and quasilinear control to stabilize a more complex model, including tether deformations. In this paper, pseudolinear control laws are presented and applied to a simple point-mass model. Numerical examples calculated use system parameters representative of the planned Italian-American TSS mission.[10] A clear result that emerges is that system pitch attitude measurements are critical; the currently planned 2-deg resolution in these measurements is far too coarse to permit fast efficient retrieval with automatic closed-loop stabilization. A bang-bang feedback design may change this conclusion.

Omitted from this paper is any treatment of proximity operations. Both subsatellites are modeled as point masses without attitude dynamics. Docking is defined to occur when the separation between these point masses reaches some value (taken as 10 m in numerical work). These simplifications permit use of a very simple model for the system dynamics, but it is doubtful whether the results of this study remain valid to very short tether lengths, lengths comparable to the dimension of either subsatellite.

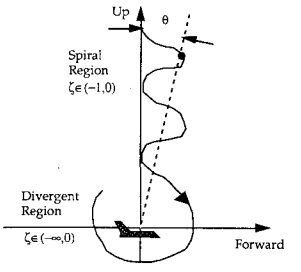

Fig. 2 In-plane trajectory.

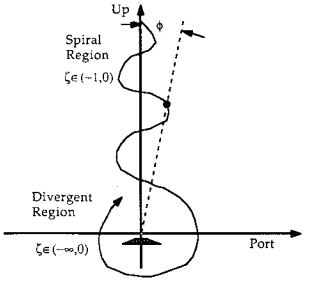

Fig. 3 Out-of-plane trajectory.

II. System Dynamics

Much of the interesting dynamics of two small satellites connected by a taut, low-mass, long tether are described[1] by three equations describing length, pitch, and roll of the system (the center of gravity of the system is in a circular orbit):

$$\ddot{L} = L\left[(\dot{\theta}+\omega)^2\cos(\phi) + (\dot{\phi})^2 + 3\omega^2\cos^2(\theta)\cos^2(\phi) - \omega^2\right] \quad (1a)$$

$$\ddot{\theta} = (\dot{\theta}+\omega)2\tan(\phi)\dot{\phi} - 2\frac{\dot{L}}{L}(\dot{\theta}+\omega) - 3\omega^2\cos(\theta)\sin(\theta) \quad (1b)$$

$$\ddot{\phi} = -2\frac{\dot{L}}{L}\dot{\phi} - \left[(\dot{\theta}+\omega)^2 + 3\omega^2\cos^2(\theta)\right]\cos(\phi)\sin(\phi) \quad (1c)$$

where L is the instantaneous length, θ the in-plane angle between the (straight) tether and the local vertical, ϕ the out-of-plane angle between the (straight) tether and the local vertical, and ω the orbital rate (circular orbit).

To understand the basic instabilities during retrieval, it is instructive to partially linearize these equations. The pitch angle θ does not remain small since it is directly driven by length changes. For $\dot{\theta},\dot{\phi} \ll \omega$, $\phi \ll 1$, the partially linearized forms of Eqs. (1a-1c) are

$$\ddot{L} = L\left[(\dot{\theta}+\omega)^2 + 3\omega^2 + 3\omega^2\cos^2(\theta) - \omega^2\right] \quad (2a)$$

$$\ddot{\theta} = -2\frac{\dot{L}}{L}(\dot{\theta}+\omega) - 3\omega^2\cos(\theta)\sin(\theta) \quad (2b)$$

$$\ddot{\phi} = -2\frac{\dot{L}}{L}\dot{\phi} - \left[(\dot{\theta}+\omega)^2 + 3\omega^2\cos^2(\theta)\right]\phi \quad (2c)$$

If the length is controlled so that $\dot{L}<0$ (retrieval), then the $(\dot{L}/L)$ term in the pitch and roll equations is negative, and both pitch and roll are negatively damped, nonlinear, second-order oscillators. There is still a small coupling from pitch into roll.

A. Pitch/Roll Dynamics

Equations (1a-1c) or (2a-2c) can be integrated forward in time for particular retrieval rates $L(t)$. The result is a set of trajectories of the subsatellite with respect to the orbiter, one for each set of initial conditions. These trajectories are three-dimensional; typically their in-plane or out-of-plane projections are displayed. Figure 2 is a sketch of the in-plane component of typical trajectories; Fig. 3 is the out-of-plane. The local vertical/horizontal reference frame is shown reference. In these figures ζ represents the damping ratio (negative for retrieval) of the fully linearized dynamics derivable from Eqs. (2a-2c) by assuming $\theta \ll 1$. The open-loop trajectories are unstable and in the final stages of the retrieval encircle the orbiter.

The most interesting dynamics occur in pitch. Two competing mechanisms drive the equilibrium ($\ddot{\theta}=\dot{\theta}=0$). Gravity gradient provides a torque restoring the configuration to the local vertical. Coriolis acceleration drives θ, depending on the product $\omega\dot{L}/L$. For low enough relative length rates, equilibrium is given by

$$\theta_{\text{EQUIL}} \cong \frac{2}{3}\frac{L}{\omega L} \quad (3)$$

and during retrieval the pitch angle oscillates with growing amplitudes about this time-varying equilibrium. We call this the spiral region.

For too large a relative length rate, Coriolis acceleration overcomes gravity gradient and no equilibrium is achieved, so that $|\theta(t)|$ is an increasing function of time. We term this the divergent region.

B. Length Dynamics

Tether length is directly controllable with the reel/deployer in the orbiter payload bay. This control authority is subject to the important physical constraint that the tension remain positive. An expression for the tension is given by (ignoring tether-aligned thrusting)

$$\frac{T}{m_s} = L\left[(\dot{\theta}+\omega)^2 + \omega^2\cos^2(\phi) + (\dot{\phi})^2 + 3\omega^2\cos^2(\phi)\cos(\theta) - \omega^2\right] - \ddot{L} \quad (4)$$

where m_s is the mass of the subsatellite. If the tension in the tether is zero at any phase during the retrieval, the tether goes slack.

III. Trajectory Design

The envisioned feedforward retrieval trajectory has several characteristics:

1) It is implemented with the tether reel only; thus, it satisfies Eqs. (1a) and (1b), with the reel providing a specified

length time history $L(t)$. Tether-normal thrusters are not used.

2) The tether tension must remain positive. This limits the rate at which one can decelerate a reel-in velocity. The deceleration force is given either by gravity gradient tension or by a tether-aligned thruster that may be present.

3) When the docking length is reached, the pitch and roll angles θ and ϕ and their rates $\dot{\theta}$ and $\dot{\phi}$ must all be practically zero.

One might formalize these specifications into a cost function or set of constraints and apply numerical methods to find an optimal trajectory. Indeed, we will report on such work, more fully presented in Ref. 11. It is useful first to consider a more heuristic discussion.

A. Heuristic Discussion of Retrieval Trajectories

Before solving for the optimal length-rate profile, it is instructive to understand the characteristics of possible optimal retrieval trajectories in both the phase plane and the local-vertical-local-horizontal (LVLH) planes. In the phase plane it is instructive to examine pitch motion (roll will be similar) for various constant values of relative retrieval rate ratios $\dot{L}/L$. Since $\dot{L}/L$ is actually time-varying, the actual phase-plane trajectories will be a continuously changing blend of those shown here.

Inspection of Eq. (2b) and comparison with the standard form for a second-order linear oscillator equation

$$\ddot{\theta} + 2\zeta\omega_n\dot{\theta} + \omega_n^2\theta = f(t) \tag{5}$$

suggests that the pitch motion will consist of growing oscillations with natural frequency

$$\omega_n = \sqrt{3}\omega \tag{6}$$

and with an exponential envelope given by

$$e^{-\zeta\omega_n t} \quad \text{where} \quad \zeta = \frac{\dot{L}}{L\sqrt{3}\omega} < 0 \tag{7a}$$

These pitch oscillations occur about the time-varying equilibrium angle $\theta_{\text{EQUIL}}(t)$ given by Eq. (3). This viewpoint remains valid for slow length changes $|\zeta| < 1$, but for rapid retrieval or for short lengths, the motion changes character; the pitch angle diverges monotonically in time. The boundary between these motions is predicted linearly by

$$\frac{\dot{L}}{L} = \sqrt{3}\omega, \qquad \zeta = -1$$

Figure 4 shows several numerically generated phase plane portraits of the pitch dynamics [Eq. (1b)] for several constant values of the damping ratio ζ. Although the equilibrium points disappear for $\zeta < -\sqrt{3}/4 = -0.433$, (the gravity gradient torque can no longer equilibrate the Coriolis torque), the phase plane portraits for $|\theta| \ll 1$ remain practically identical to those predicted by the linearized analysis. In particular, the "splitting line" in Fig. 4b is predicted by linearized analysis to be the line

$$\dot{\theta} = (\theta - 1.0)\sqrt{3}\omega \tag{7b}$$

This is clearly a good approximation for $|\theta| \ll 1$.

With the insight afforded by these phase plane sketches, it is possible to infer characteristics of the retrieval trajectory shortly before docking at $\ddot{\theta} = \dot{\theta} = 0$. Since the relative length rate ratio $(\dot{L}/L)$ commanded by the tether-reel-in controller appears explicitly in the damping term of the pitch dynamics, there can exist at most three possible optimal retrieval path scenarios:

1) The phase plane trajectories can remain strictly spirally divergent, $(|\zeta| < 1)$. This would correspond to an oscillatory retrieval with many cycles occurring before docking. Such trajectories correspond to very slow retrievals, with length decreasing exponentially in time.

2) The phase plane trajectories can be strictly divergent, $(|\zeta| > 1)$. This applies to a restricted class of initial conditions, which all begin with $\theta > 0$, $\dot{\theta} < 0$. Retrieval along such nominal paths are fast and are only possible if $L_i < \dot{L}_{\max}/\omega$.

3) The optimal retrieval path can be a composite blend of the spiral and divergent dynamics. For part of the retrieval the pitch dynamics are oscillatory. The final segment, however, diverges as it approaches the final docking condition.

Of the three possible optimal retrieval scenarios, the third is the most general and is likely to occur for typical initial lengths and length speed limits $|\dot{L}_{\max}|$. Since the desired docking conditions are taken to be zero pitch angle and pitch rate, the final approach path that each composite optimal trajectory follows can be displayed in the phase plane by realizing that, shortly before docking, the trajectory will become divergent when ζ becomes -1. Assuming a constant velocity for this short portion of the retrieval (we call this portion the "final approach path"), the duration of the approach path can be approximated from the following equation:

$$t_{\text{approach}} = \frac{L_f - L_{\text{switch}}}{\dot{L}} \tag{8}$$

where L_{switch} is the length of the tether when spiral trajectories become divergent. From the phase plane analysis presented earlier, this transition occurs when $\zeta = -1$ or when

$$L_{\text{switch}} \cong -\frac{\dot{L}}{\sqrt{3}\omega} \tag{9}$$

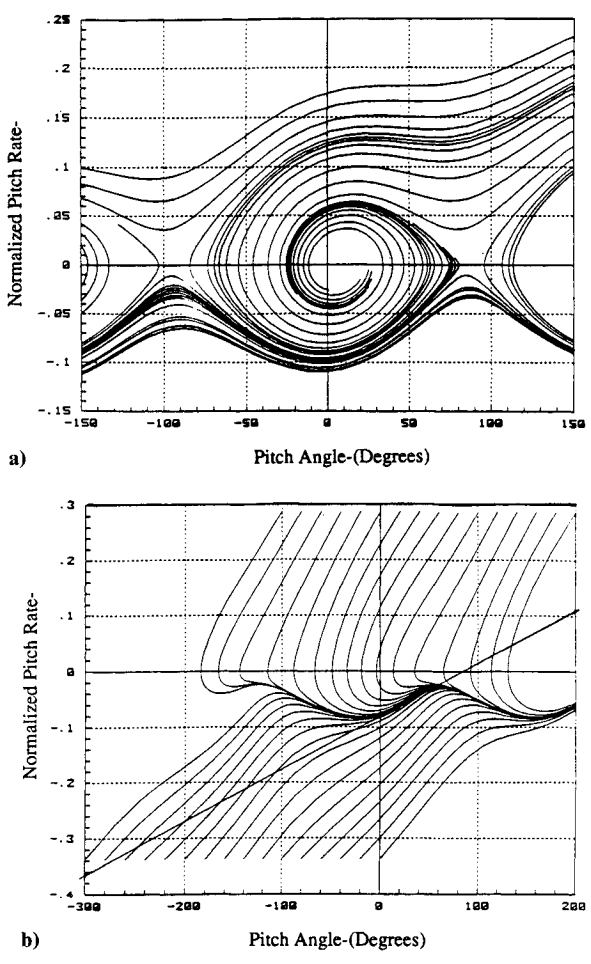

Fig. 4 Pitch phase plane portraits for specific values of the damping ratio ζ: a) $\zeta = -0.10$, b) $\zeta = -0.70$.

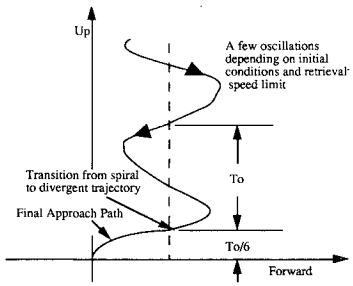

Fig. 5 A typical retrieval that ends with little pitch, and pitch rate terminates on an invariant final approach path. This final approach is preceded by a number of diverging oscillations, the number depending primarily upon the initial length and the maximum allowable retrieval rate. T_o is the period of natural oscillation.

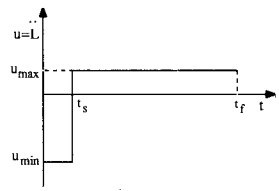

Fig. 6 The length acceleration will be bang-bang during the final retrieval with maximum allowable values. Only one switch is anticipated.

where L_f has been taken to be zero. Substituting for L_{switch} in Eq. (8) and assuming that L_f is negligible, the duration of the final approach trajectory is

$$t_{\text{approach}} = \frac{1}{\sqrt{3}\omega} \tag{10}$$

Analysis of the phase plane for $\zeta = -1$ implies that, at the instant of switching to divergent dynamics, pitch angle and pitch rate are approximately

$$\theta = 1 \text{ rad}, \qquad \dot{\theta} = -0.16\omega \tag{11}$$

To achieve this desired approach path from any arbitrary initial condition, the retrieval trajectory may undergo a few oscillations as length rate is adjusted to all of the system trajectory along the final approach path (see Fig. 5). The number of oscillations required will depend on the initial length and the maximum allowable retrieval speed, since these two parameters approximately specify the retrieval duration. However, retrieval is not possible from all initial conditions. For those initial conditions beginning outside the circle defined by

$$\theta_i^2 + \left(\frac{\dot{\theta}}{\sqrt{3}\omega}\right) = 1 \tag{12}$$

convergence cannot be achieved unless the tether is first lengthened to slow down the pitching motion.

B. Formal Trajectory Optimization

Assuming that the tether-reel can be commanded to track a specific length profile $L(t)$, one way to restrict the behavior of the retrieval near docking is to find the nominal length $L(t)$ that forces the pitch dynamics along an equilibrium path all of the way to the final docking conditions. In addition, the tether reel must enforce retrieval such that the tether tension remain positive (no pushing allowed): 1) $T(t) > 0$, and the impact speed not exceed some safe limit: 2) $-\dot{L}_{\max} < \dot{L}(t_f) < 0$.

This can be done by formulating a quadratic cost of the following form

$$J(t_f) = \phi[x(t_f), t_f]$$
$$= \dot{\theta}(t_f)^2 + \left(\frac{\dot{\theta}}{\omega}\right)^2 + \left(\frac{\omega t_f}{2\pi}\right)^2 + \alpha\dot{L} \tag{13}$$

where $\alpha > 0$ is a penalty used to ensure that constraint 2 is met. To be able to take into account inequality constraint 1 on the tension, the control must appear either in the expression for T, Eq. (4), or in its derivatives (see Ref. 12). Since T depends on the second derivative of the length, the control $u(t)$ is taken to be the acceleration $\dot{L}(t)$. Choosing a state-space realization for the system dynamics with the state vector x defined as

$$x^T = [x_1\ x_2\ x_3\ x_4]^T = [\theta\ \dot{\theta}\ L\ \dot{L}]^T$$

allows writing the pertinent dynamic equations in first-order state space form:

$$\dot{x} = f(x,u) \tag{14}$$

Where the 4×1 vector $f(x,u)$ is the state space representation of Eqs. (2a) and (2b), the optimal retrieval problem can be stated as follows: find the control history $u(t)$ that maximizes the Hamiltonian $H(x,u,t)$ given by

$$H = \lambda^T f(x,u) - \mu T \tag{15}$$

where λ are the costates, and $\mu = 0$ if $T > 0$ or $\mu > 0$ if $T \le 0$. The first derivative of the Hamiltonian with respect to the control u is given by

$$H_u = \lambda_4 + \mu \tag{16}$$

where λ_4 is the costate associated with the length rate x_4. H_u does not depend on the control. Consequently, the control is bang-bang. If $\lambda_4 + \mu > 0$, then $u = u_{\max}$. On the other hand, if $\lambda_4 + \mu < 0$, then $u = u_{\max}$. At the beginning of the retrieval, typically $u = u_{\min}$ in order to accelerate the subsatellite toward the orbiter. $|u_{\min}|$ is determined by the allowable tension that the tether system can impose, whereas $u_{\max}$ should be chosen to be a value safely below the acceleration that will cause the tether to become slack. If $\dot{\theta}$ and θ are small, the constraint on the tension may be written as (for the tether aligned thrusting):

$$T(t) = 3\omega^2 L - \ddot{L} > 0 \tag{17}$$

Therefore, the constraint will never be violated as long as

$$\ddot{L} < 3\omega^2 L_f = u_{\max} \tag{18}$$

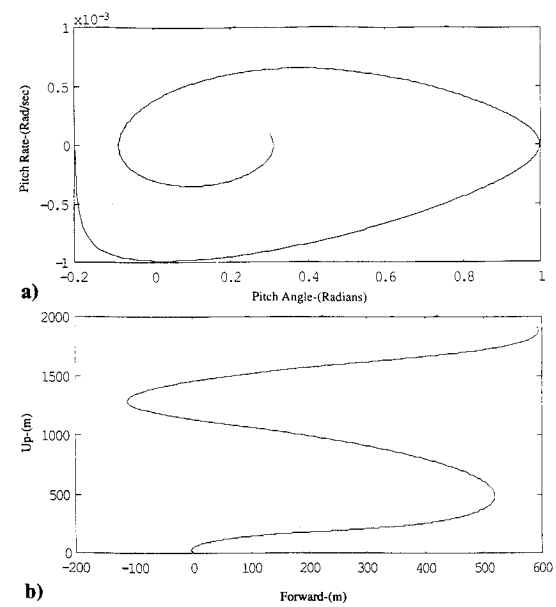

Fig. 7 Optimal phase plane trajectory (a) and optimal in-plane trajectory (b).

If we adapt values for u_{max} and u_{min} that are invariant with time, then the optimal control will consist of a set of switch times from $\dot{L}(t)=u_{max}$ to $\dot{L}(t)=u_{min}$. The simplest retrieval (and also perhaps intuitively obvious) involves only one switch; retrieval begins with maximum acceleration toward the orbiter and continues with a long period of maximum deceleration to slow down for docking. The simplest optimization will then consist of selecting only the one unknown parameter, the switch time t_s. That this simplification is valid has been confirmed numerically by solving the two-point boundary value problem, with results presented in Ref. 11.

C. Representative Trajectories

The preceding analysis has argued that a sensible trajectory would employ maximum allowable length acceleration and deceleration and that only a single switch would occur; the retrieval begins with a short acceleration and then decelerates for the entire remaining time at the maximum allowable rate so that docking occurs with an acceptable impact speed. Figure 6 makes this statement graphically. The figure includes the assumption that the acceleration limits are constant, independent of length, and we have used this assumption in numerical examples. The acceleration time history must be such that the docking speed (when $L=L_f$) is in the range $\dot{L}_f \in (\dot{L}_{f\max}, 0)$. Thus, $t_{s\min} \le t_s \le t_{s\max}$ with

$$t_{s\min} = \sqrt{\frac{\left(\frac{\dot{L}_{f\max}}{u_{max}}\right)^2 + \frac{2}{u_{max}}(L_o - L_f)}{\left(\frac{u_{min}}{u_{max}}\right)^2 - \frac{u_{min}}{u_{max}}}}$$

$$t_{s\max} = \sqrt{\frac{\frac{2}{u_{max}}(L_o - L_f)}{\left(\frac{u_{min}}{u_{max}}\right)^2 - \frac{u_{min}}{u_{max}}}} \qquad (19)$$

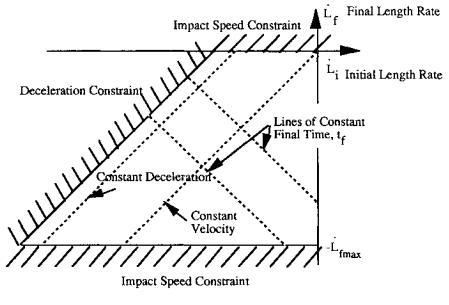

Fig. 8 Feasible region for constant acceleration retrieval, in which the initial and final length rates parameterize the retrieval.

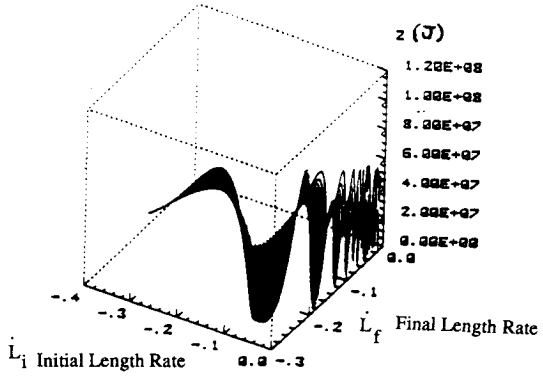

Fig. 9 Cost function for constant acceleration retrieval, particular initial condition.

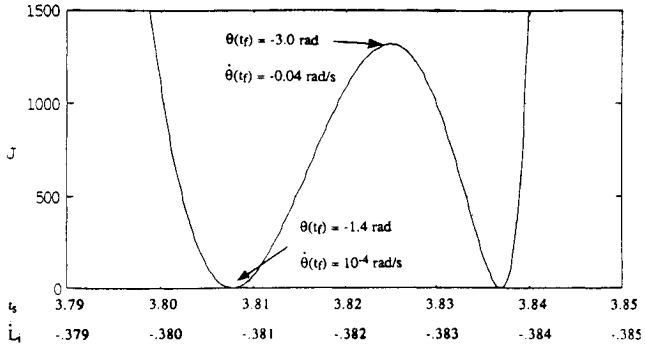

Fig. 10 Zoom of cost function in region of first minimum for a constant deceleration retrieval, with initial conditions defined in the text.

The stopping condition is $L(t)=L_f=10$ m. For an optimal t_s, the total time of retrieval t_f is given by

$$t_f = t_s - \frac{u_{min}}{u_{max}} t_s - \sqrt{\left[\left(\frac{u_{min}}{u_{max}}\right)^2 - \frac{u_{min}}{u_{max}}\right] t_s^2 - \frac{2}{u_{max}}(L_o - L_f)} \qquad (20)$$

and the impact velocity by

$$\dot{L}_f = -u_{max} - \sqrt{\left[\left(\frac{u_{min}}{u_{max}}\right)^2 - \frac{u_{min}}{u_{max}}\right] t_s^2 - \frac{2}{u_{max}}(L_o - L_f)} \qquad (21)$$

A computed example follows, with numerical parameters relevant to the final 2-km retrieval of the Italian-American TSS.[10] We take arbitrary initial conditions, $L_i=2000$ m, $\theta(0)=0.3$ rad, and $\dot{\theta}(0)=0.1\omega$ rad/s, and somewhat arbitrary constraints, $u_{min}=-0.1$ m/s^2, $u_{max}=3\times10^{-5}$ m/s^2, and $\dot{L}_{f\max}=-0.5$ m/s. Docking is defined to occur when $L=L_f=10$ m. The optimal retrieval [in the sense of minimizing the cost, Eq. (13)] uses $t_s=3.84$ s; the reel accelerates in the first 3.84 s to a retrieval velocity of $\dot{L}_f(t_s)=-0.384$ m/s and decelerates uniformly thereafter, docking with an impact velocity of -0.17 m/s. The retrieval duration is 7300 s, 1.15 orbits.

Figure 7 shows the retrieval trajectory in the phase plane and in the local vertical/local horizontal coordinates. The subsatellite performs one period of pitch oscillation before starting the final approach. The maximum pitch excursion is 1 rad and occurs just before the trajectory enters the approach corridor.

The final path leaves the "splitting line" too late to be able to reach the point (0,0) in the phase plane. In this case, $\theta_f=-0.20$ rad and $\dot{\theta}_f=-4.44\times10^{-5}$ rad·s^{-1} with $\dot{L}_f=-1.67$ m·s^{-1}. It turns out that the optimal problem as stated does not enable us to reach our target point (0,0).[11]

D. Open Loop Sensitivity

The preceding section has argued that the length rate, for constant acceleration constraint, will be a linear function of time. The very brief period of initial acceleration (3.84 s in the computed example) is negligible; one can approximate the length time history as beginning at $t=0$ with an initial speed $\dot{L}(0)=(u_{min}*t_s)$, followed by a constant deceleration. Figure 8 sketches the feasible region, parameterized by initial and final retrieval rates. The shape of the cost function in this region with the initial conditions $\theta(0)=0.3$ rad and $\dot{\theta}(0)=0.1\omega$ rad·s^{-1} is given by Fig. 9. This three-dimensional plot of the cost function shows that peaks and valleys alternate. The valleys almost follow the direction of constant retrieval time. In fact, each valley corresponds to the number of orbits the path performs in the phase plane in the spiral region.

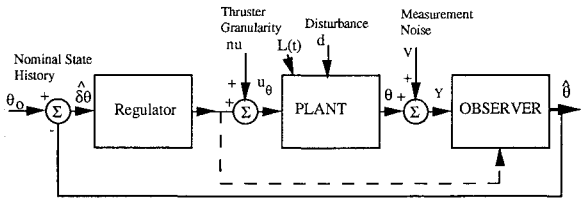

Fig. 11 A linear time-varying feedback control loop.

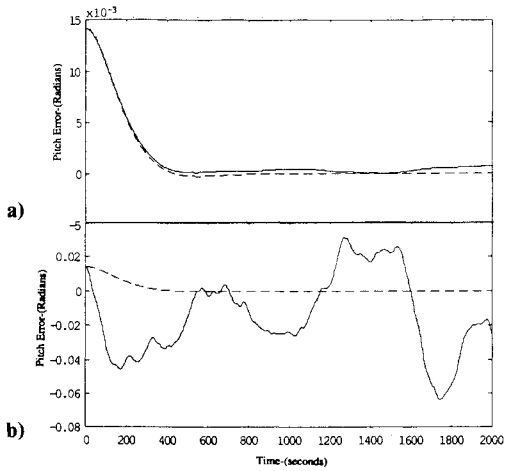

Fig. 12 Comparison of LQG closed-loop pitch retrieval response with slow (a) and fast (b) estimators. A 1% error in the pitch initial conditions is assumed.

A minimum time recovery corresponds to a minimum number of orbits, which is one. Visual inspection of Fig. 9 leaves the impression that the first valley is the "broadest," suggesting that fastest possible retrieval will be the least sensitive.

The unstable nature of the system results in a high sensitivity of the trajectory to parameter variations. Figure 10 gives a zoom of the cost function in the region of the first minimum. Note that a 1% variation in the switch time (alternatively, the initial retrieval speed) leads to very different costs and also to very different trajectories. The retrieval instability is such that the tolerance on retrieval parameters for open-loop retrieval is unrealistically small. Most of this sensitivity is due to the very strong instability in the final phases of the retrieval, when the trajectory is balancing along the splitting line of the phase portraits of Fig. 4.

This high sensitivity to small errors in retrieval trajectory and initial conditions supports the use of tether-normal thrusters to force the subsatellite along the nominal retrieval path all of the way to docking. Furthermore, since the initial conditions are unlikely to be determined to within 1% and the retrieval rates cannot be controlled as tightly either, there is little practical utility in calculating optimal retrieval trajectories that depend upon fine details of the initial conditions. Rather, it would be useful to precalculate a few nominal retrieval trajectories, each suboptimal but approximately applicable to some large portion of the space of initial conditions. These retrieval trajectories each would be specified by a few parameters. In operation, upon observation of the approximate initial conditions, one of these feedforward trajectories would be selected, and feedback would be used to drive the actual trajectory toward this nominal one.

IV. Feedback Stabilization

The preceding section has discussed nominal retrieval trajectories and the need for feedback stabilization. Figure 11 presents our concept of this feedback loop. Here the "plant" represents the perturbational dynamics in pitch and in length. For purposes of feedback control design, we view these dynamics as linear time-varying and consider the coupling between length and pitch. This coupling is two-way, but the most important direction, particularly for short lengths, is from length dynamics into pitch dynamics. Any length maneuvers—say, due to length disturbances or due to length sensor noise—then drive the pitch dynamics. In spite of this, the feedback control presented in this paper is based on the assumption of decoupled dynamics. For a more complete discussion of this point and for feedback design for the coupled dynamics of pitch and length perturbations, refer to Ref. 11.

A. Pitch Dynamics Feedback Stabilization

With reference only to pitch dynamics, the plant in Fig. 11 satisfies (where θ and $\dot{\theta}$ are now perturbational quantities)

$$\begin{bmatrix}\dot{\theta}\\ \ddot{\theta}\end{bmatrix} = \begin{bmatrix}0 & 1\\ -3\omega^2\cos\left[2\theta_N(t)\right] & -2\omega\dfrac{\dot{L}_N(t)}{L_N(t)}\end{bmatrix}\begin{bmatrix}\theta_N\\ \dot{\theta}_N\end{bmatrix} + \begin{bmatrix}0\\ \dfrac{1}{L_N(t)}\end{bmatrix}u \tag{22}$$

where $\theta_N(t)$, $\dot{L}_N(t)$, and $L_N(t)$ are the nominal pitch, length rate, and length time histories and u_θ the translational acceleration of the subsatellite due to tether-normal thrusting. Although only system attitude θ can be directly measured, here we discuss full state feedback and postpone discussion of sensors and state estimation to a subsequent section.

The perturbational dynamics are linear but time-varying. If one intends to gain schedule, then linear feedback of the form

$$u_\theta = g_p\theta + g_d\dot{\theta} \tag{23}$$

can be used for pole placement. A choice of

$$g_p(t) = L_N(\omega_c^2 - 3\omega^2\cos 2\theta) \tag{24a}$$

$$g_d(t) = L_N\left(2\delta\omega_c - 2\omega\frac{\dot{L}_N}{L_N}\right) \tag{24b}$$

leads to time-invariant closed-loop perturbational pitch dynamics with a damping ratio of δ and a crossover frequency ω_c. Note the explicit time dependence of these feedback gains; they tend to decrease with the length, offsetting the increase in pitch control authority of the tether-normal thruster. Values of $\delta = 0.70$ and $\omega_c = 10^{-2}$ rad/s are reasonable first guesses for the desired closed-loop dynamics. The closed-loop bandwidth, roughly ω_c, must be selected as a compromise between pitch sensor noise and disturbance rejection. Another limiting factor is the desire to avoid actuator saturation in response to errors in initial conditions.

For the purpose of linear regulator design, it would be convenient to be able to command a continuously varying level of thrust. The available thrusters for the TSS are on-off devices, but continuous thrust level may be approximated by fast pulsing with pulse width modulation. The pulsing period ΔT must be short compared with the system characteristic time constant so as to approximate reasonably the effect of continuous thrusting. If $u_\theta(t)$ is the continuous acceleration level commanded by the regulator and u_s the constant acceleration level available, the firing duration Δt for a pulsing interval ΔT is given by

$$\Delta t = \frac{1}{u_s}\int_0^{\Delta T} u(t)\,dt \tag{25}$$

yielding the same impulse. Since Δt is lower than ΔT, the average value of requested thrusting must always be lower than the available constant thrust level. Simulations reported in Ref. 11 have shown that pitch errors as small as 1 deg at a

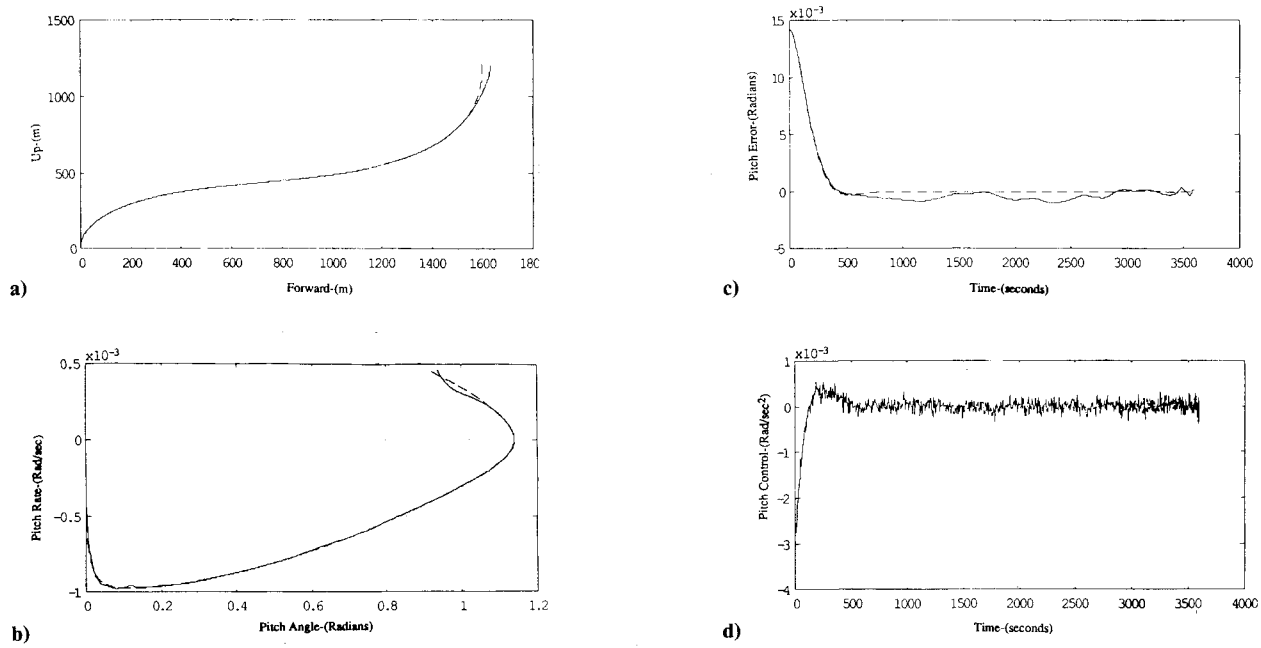

Fig. 13 Nonlinear retrieval simulation using gain scheduled LQG methods with an extended Kalman filter to update estimator gains throughout the duration of the retrieval. Simulation results shown for a 1% error in pitch initial conditions: a) in-plane trajectory, b) phase plane trajectory, c) pitch error with respect to nominal trajectory, and d) pitch control history along the retrieval.

length of 2 km during a typical retrieval will lead to feedback commands that saturate this thruster. This suggests that the feedback bandwidth may have to be reduced, although the chosen value of $\omega_c = 10^{-2}$ is already only 10 times slower than the typical retrieval duration.

B. Pitch Sensing and State Estimation

The envisioned pitch sensing system on the Italian-American TSS employs orbiter-based line-of-sight measurements to the subsatellite together with knowledge of the orbiter LVLH attitude. The line-of-sight sensor is a Ku band radar, with a resolution of ± 2 deg,[13] much worse than the uncertainty in the orbiter attitude. This section investigates the possibility of extracting reasonable state estimates for θ and $\dot{\theta}$ from this sensor. Traded against this measurement noise are errors in the plant model, nonzero initial errors in the state estimates, and a disturbance spectrum that we here attribute entirely to unpredictable thrust granularity.

We would like to use Kalman filter theory to make an optimal choice in the trade between sensor noise and plant disturbances. To this end, we convert the sensor specification of 2 deg precision into an "equivalent white noise" with a variance of $\frac{1}{3}$ deg^2 (Ref. 14). Gas jets on the subsatellite give a constant thrust of $2N$ nominal. For a total mass $m = 500$ kg, the resulting acceleration is $u_s = 4 \times 10^{-3}$ m·s^{-2}. The time granularity of this on-off system is 80 ms, leading to a Δv granularity 3.2×10^{-4} m·s^{-1} per thrust pulse. To turn this into an acceleration disturbance requires knowledge of the thrust pulse interval ΔT. Here we arbitrarily assume a very high acceleration disturbance of 8.5×10^{-7} m^2·s^{-4} and, thus, an equivalent "white noise disturbance" with a variance of $3.2 \times 10^{-4}/2.58$ m·s^{-2}.

Inserting these values into the perturbational dynamics [Eq. (22)] and solving for the steady-state Kalman estimator yields heavily damped estimator poles of $(-0.8 \pm 0.9i) \times 10^{-2}$ rad/s comparable to the anticipated closed-loop bandwidth.[11] Were we to use more realistic, lower levels of acceleration disturbance, these estimator poles would be even slower. This means that the estimator ignores the sensor and relies almost entirely on the dynamics to reconstruct the states. This is due to the fact that plant noises are small compared with sensor noises.

It is tempting arbitrarily to assign estimator dynamics to be much faster. This goal must be tempered by the realization that the state estimates will be correspondingly sensitive to sensor noise. Reference 11 compares the preceding estimator with one 25 times faster (poles at $-0.2 \pm 0.2i$ rad·s^{-1}), in a linear time-varying simulated retrieval in which only the perturbational dynamics [Eq. (22)] are modeled. In this simulation, the closed-loop response with the slow estimator is much more acceptable than with the fast estimator. Steady-state pitch excursions are lower (below 0.1 deg), and the suppression of initial condition errors are acceptable (Fig. 12a). The fast estimator leads to large pitch excursions (several degrees), larger than the sensor resolution and larger than the 1-deg initial condition being simulated (Fig. 12b). The feedback control system responds almost only to sensor noise, even amplifying it.

V. Nonlinear Retrieval Simulation

This section reports a simulation of pitch dynamics, based on the nonlinear equation of motion, Eq. (1b). The feedforward trajectory is imposed as discussed in Sec. III, with an initial brief interval (approximately 6 s) of high tension, followed by a long interval of constant, slight deceleration. Docking occurs after about 0.57 orbits (3600 s) with a docking speed of 0.5 m·s^{-1}. The estimator uses the nonlinear equation of motion [Eq. (1b)], but new Kalman estimator gains are computed along the retrieval trajectory, based on the linear perturbational dynamics of Eq. (23) and ignoring the time variation in these dynamics. The slow estimator of Sec. IV.B is employed.

Initial conditions are $\theta_N(0) = 53$ deg, $\dot{\theta}_N(0) = 4.5 \times 10^{-4}$ rad·s^{-1} (0.39 times orbital rate), $L_N(0) = 2000$ m, and $\dot{L}_N(0) = 0.0$. Initial conditions on the perturbations are $\theta(0) = 0.8$ deg, $\dot{\theta}(0) = 9.7 \times 10^{-6}$ rad·s^{-1} (about 1% of orbital rate), $L(0) = 20$ m, and $\dot{L}(0) = 6 \times 10^{-3}$ m·s^{-1}. The pitch dynamics are feedback stabilized, as discussed previously.

Figures 13a–13d present simulated results. Although the performance indicated by these simulated results is encouraging (the initial pitch error decays without overshoot and thereafter stays less than 0.05 deg), the control effort expanded is unacceptably high. Figure 13d indicates that the pitch control thruster is firing continually, consuming fuel in the amount of 680 m·s^{-1}, much greater than the 2 m/s saved by introducing the feedforward nominal retrieval trajectory.

These results suggest several things:

1) The pitch sensor should be drastically improved.

2) The feedback bandwidth might be reduced, but errors in initial conditions will decay more slowly.

3) A feedback limit cycle design similar to that reported in Ref. 8 seems promising. The deadband chosen should take both thruster and pitch sensor characteristics into account.

VI. Summary

The major contribution of this paper is the suggestion that tether retrieval maneuvers be guided by a strategy of trajectory planning, feedforward, and feedback stabilization. The tether reel should be used as the feedforward actuator, establishing a nominal but unstable retrieval trajectory. Tether-normal thrusting should be used for feedback stabilization.

The paper has presented a first pass through the entire retrieval problem. For fast retrieval without spinup of the tethered system, we report an invariant final approach corridor that the trajectory must follow. We suggest some strategies for generating nominal retrieval trajectories and compute several from arbitrary initial conditions. Retrieval times of less than one orbit are typical, with the limitation on retrieval time given primarily by limits on docking speed and limits on length rate deceleration (tether tension).

Feedback stabilization of the pitch dynamics during retrieval is based upon the linear time-varying perturbational dynamics. The paper presents pseudolinear control designs, using gain-scheduled state estimation from a noisy pitch sensor and gain-scheduled feedback of these state estimates to a tether-normal thruster. The thruster uses pulse-width modulation to imitate continuous control. Several conclusions emerge:

1) The resolution of 2 deg in the pitch sensor should be much improved.

2) The arbitrarily chosen feedback bandwidth of 10^{-2} rad$\cdot$s^{-1} may be too high.

3) The feedback design should be repeated using bang-bang techniques to design a limit cycle.

This paper suffers from using too simple a model of the dynamics. An important neglected effect is the internal flexible dynamics of the tether, particularly with bang-bang thruster maneuvers of the subsatellite. Also important but neglected in this paper are the attitude dynamics of the subsatellites, particularly during proximity operations and during docking impact.

Acknowledgment

The authors would like to thank the Rotary International Foundation for providing support for this research.

References

[1]Misra, A. K., and Modi, V. J., "Dynamics and Control of Tether Connected Systems—A Brief Review," 33rd Congress of the International Astronautical Federation, Paper 82-315, Paris, Sept. 1982.

[2]von Tiesenhausen, G., "Tethers in Space—Birth and Growth of a New Avenue to Space Utilization," NASA TM-82571, Feb. 1984.

[3]Misra, A. K., and Diamond, G. S., "Dynamics of a Subsatellite System Supported by Two Tethers," *Journal of Guidance, Control, and Dynamics,* Vol. 9, No. 1, 1986, pp. 12–16.

[4]Misra, A. K., Xu, D. M., and Modi, V. J., "On Vibrations of an Orbiting Tether," *Acta Astronautica,* Vol. 13, No. 10, 1986, pp. 587–596.

[5]Rupp, C. C., "A Tether Tension Control Law for Tethered Subsatellites Deployed Along Local Vertical," NASA TMX-64963, Sept. 1975.

[6]Baker, W. P., "Tethered Subsatellite Study," NASA TMX-73314, March 1976.

[7]Bainum, P. M., and Kumar, V. K., "Optimal Control of the Shuttle-Tethered System," *Acta Astronautica,* Vol. 7, No. 12, 1980, pp. 1333–1348.

[8]Pines, D. J., von Flotow, A. H., and Redding, D. C., "Two Nonlinear Control Approaches for Retrieval of Tethered Thrusting Subsatellite," *Journal of Guidance, Control, and Dynamics,* Vol. 13, No. 4, 1990, pp. 651–658.

[9]Xu, D. M., Misra, A. K., and Modi, V. J., "On Thruster Augmented Active Control of a Tethered Subsatellite System During Its Retrieval," AIAA Paper 84-1993, Aug. 1984.

[10]Crouch, D. S., and Vignoli, M. M., "Shuttle Tethered Satellite System Development Program," AIAA Paper 84-1106, June 1984.

[11]Fleurisson, E. J., "A Feedforward/Feedback Approach to Retrieval of a Tethered Sub-Satellite," S.M. Thesis, Dept. of Aeronautics and Astronautics, Massachusetts Inst. of Technology, Cambridge, MA, Aug. 1990.

[12]Bryson, A. E., and Ho, Y. C., *Applied Optimal Control,* Hemisphere, New York, 1975, Chap. 7, Sec. 9.

[13]Bodley, C., Dynamics and Control engineer at Martin Marietta, personal communication, June 1990.

[14]Franklin, G. F., Powell, J. D., and Emanmi-Naeini, A., *Digital Control of Dynamic Systems,* Addison-Wesley, Menlo Park, CA, 1980, Chap. 7.